An artificial skin for shaving applications

An artificial skin for shaving applications

A first investigation

Marjolein Jansen (E.U.T. identity number 319663)

WFW 95.094
Practical training at Philips Research Laboratories
15.04.95 - 15.07.95

supervised by
F. Starmans (Philips Research Laboratories)
C. Oomens (Eindhoven University of Technology)

Contents

1. Introduction

Research is done at Philips Research Laboratories to obtain a better performance of shaving apparatus. Various kinds of experiments related to performance are often done on persons however the use of persons for measurements causes many problems. Measurements on persons have a poor reproducibility and are hard to carry out. Some experiments are not possible to carry out in vivo, because they last too long or they are destructive. These difficulties caused the idea of an artificial skin. This should be a tissue or a material with the mechanical properties of skin. Great advantages of such an artificial skin would be the ease to experiment on it and a good reproducibility. Of course it will be difficult to find a tissue or material that has all the mechanical properties of skin. So the most important mechanical properties for this application have to be selected. It is obvious that an artificial skin can not eliminate the use of test persons, but it can however reduce the number of experiments on persons. Besides for the experiments which can't be carried out in vivo, an artificial skin can be a solution. In this way the laboratory skin can expand the possibilities to experiment.

The target of this practical training is to form a rough picture of an artificial skin for shaving applications. An artificial skin is to be developed to characterise some important mechanical properties and compare these properties to those of human skin.

This report starts with a short review of the structure of skin and hair. After that a mechanical analysis of shaving processes is given and an explanation is given of the mechanical properties, which are nearer studied: rotation friction, translation friction and static and dynamic indentation characteristics. Then the silicon materials and the thereof build artificial skin samples are introduced. Next the experimental techniques used are described, followed by the results of these experiments. Finally the results are discussed and some conclusions and recommendations drawn.

2. Structure of skin and hair

2.1 Skin

The skin is approximately 1.5 mm thick and has a stratified structure consisting of two main layers: an epidermis and a dermis. The epidermis is very thin compared to the dermis (Figure 1).
The epidermis is the exterior layer of skin, which is composed of cells and cellular debris. A continual reproduction of epithelial cells at the boundary with the dermis causes migration towards the external surface. The cells keratinise as they migrate.
The dermis supports the epidermis and consist mainly of dense networks of the fibrous proteins collagen, reticulin and elastin permeated by a semigel matrix of ground substance. In this structure there are a lot of irregularities like blood vessels, lymph vessels, hair follicles, sweat glands, nerve endings and small hair muscles.
Skin differs considerably between persons and body sites.

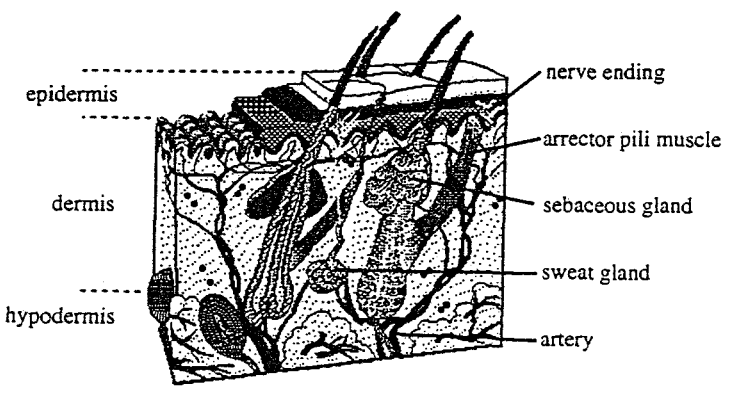

Figure 1 Structure of skin with hairs

2.2 Hair

Skin contains introversions, called hair follicles. They are slightly angled to the skin. In these follicles hairs are embedded. Hair exists of hard keratin, which expands at the hair root by dividing cells.

3. Mechanical analysis of shaving processes

Different aspects of the shaving process can be distinguished: the macroscopic contact behaviour of shaving apparatus, the microscopic contact behaviour, capturing and cutting hairs in shaving openings.
The macroscopic contact behaviour of shaving apparatus involves the translating movement of the apparatus on the skin surface. Examining this aspect it establishes that friction between skin and the surface of the apparatus is important. But also in-plane stiffness and indentation stiffness play an important part in the contact behaviour on macroscopic scale.
The contact behaviour can also be observed on microscopic scale. On this scale doming of the skin is perceived. For this protrusion, microscopic behaviour of the skin is important.
To be able to shave a hair, the shaving apparatus first has to catch a hair in one of the shaving openings. For this action again the friction between skin and the shaving apparatus is important. Besides friction the behaviour of the hair is involved as well.
Within the current project it was decided to concentrate on macroscopic contact behaviour. As in this behaviour skin friction plays a central part, it was started *analysing skin friction.*

3.1 Skin friction

Skin is very elastic compared to metals. When an elastic material is pressed against a textured rigid base the more flexible surface adapts to the contour of the other. Moving an elastic material relative with regard to a rigid base causes friction. This dry friction can be divided in an adhesive part and a deformative or hysteresive part (Figure 2). The friction force F, scaled to the normal force W, is defined as the friction coefficient f.

$$f = \frac{F}{W}$$

This coefficient can be split up into an adhesive $f_{ADHESIVE}$ and a hysteresive friction coefficient $f_{HYSTERESIVE}$, assuming that there is no interaction between these two:

$$f = f_{ADHESIVE} + f_{HYSTERESIVE}$$

With for the adhesive and hysteresive friction coefficients:

$$f_{ADHESIVE} = \frac{F_{ADHESIVE}}{W}$$

$$f_{HYSTERESIVE} = \frac{F_{HYSTERESIVE}}{W}$$

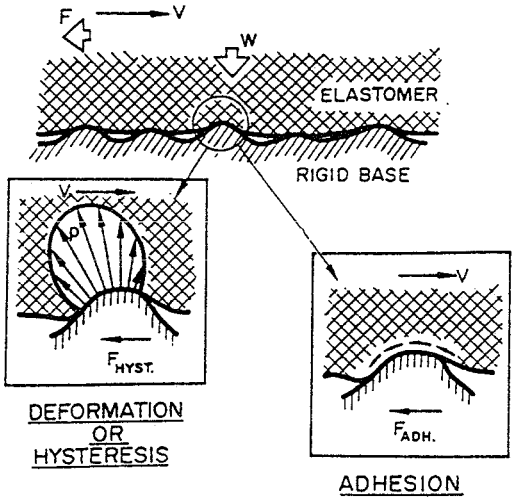

Figure 2 The adhesive and hysteresive parts of friction between elastic and rigid material (Moore 1975)

3.1.1 Adhesive Friction

The adhesive friction involves the effect of sticking surfaces. On molecular level a stick-slip process is responsible for adhesion. Molecules from the different surfaces form junctions, that offer resistance. Sliding causes these bonds to stretch, rupture and relax.
Assuming on macroscopic scale that the actual contact area between elastic and rigid material is A, with shear strength s and W the normal load, it follows for the adhesive friction coefficient (Moore 1975):

$$f_{ADHESIVE} = \frac{As}{W}$$

3.1.2 Hysteresive friction

The hysteresive friction implies friction as a result of deformation of the elastic surface. When there is no relative motion between the surfaces, the elastic

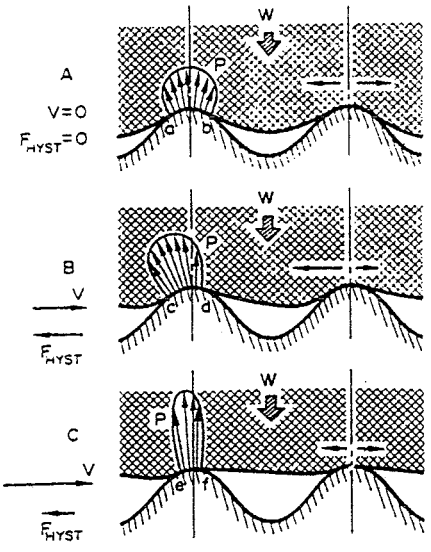

Figure 3 The dependence of velocity of hysteresive friction (Moore 1975)

material drapes symmetrical on the rigid base (Figure 3). Adding the horizontal pressure components of the deformation distribution along the rigid base, it is noticed that there isn't an effective deformational friction force. If on the other hand one of the surfaces moves with regard to the other, due to dissipative effects it occurs an asymmetrical pressure distribution, that causes in horizontal direction an effective deformational friction force. Raising the sliding speed, a more symmetrical pressure distribution develops through which the deformational friction force reduces. This deformational friction can arise because of the inertia of the test material, the damping of the test material or the adhesion friction. In the theory described in the sequel, it is assumed that damping is the dominating reason for the existence of the hysteresive friction force. This theory is based on contact between elastic material and a rigid body with many asperities with a well defined shape to model the roughness of the rigid body surface.
Moore (1975) described a hysteresive friction theory for a rigid surface with many asperities, that plough through weak rubber. When only global forms were taken into account the probe could be taken as one large asperity. At constant temperature and speed the hysteresive friction coefficient due to a rigid surface asperity can be written as:

$$f_{HYSTERESIVE} = C\left[\frac{W}{EA}\right]^{n} \tan\delta$$

Where C is dependent on the geometry of probe, Poisson's ratio ν and Young's modulus E of the elastic material. Tan δ is the loss modulus of the elastic material which characterises its dissipative behaviour and n is a constant (two or three), dependent on the probe geometry. The indentation depth w is as follows (Moore 1975):

$$w = K\left[\frac{W}{EA}\right]^{m}$$

The constant m (one or two) and the constant K are determined by the probe geometry, Poisson's ratio ν and Young's modulus E. The hysteresive friction coefficient and the indentation depth show dependency on the same ratio, W/EA. If the indentation depth increases the hysteresive friction coefficient also heightens. This is comprehensible, because the deformation increases and so the hysteresis grows, through which the hysteresive friction coefficient gets larger.

3.1.3 Total friction force

As mentioned before the total friction force consists in the current case of an adhesive and an hysteresive part. If no interaction between the adhesive and hysteresive friction is assumed, the separated friction coefficients can be added to obtain the total friction coefficient.

$$f = f_{ADHESIVE} + f_{HYSTERESIVE} = \frac{As}{W} + C\left[\frac{W}{EA}\right]^{n} \tan\delta$$

The adhesive and the hysteresive friction coefficient react contrary to changes in the actual contact area *A* and changes in the normal force *W*. Lowering the actual contact area and heightening the normal force results in a smaller adhesive friction coefficient and a larger hysteresive friction coefficient. Whether the total friction force owing to this increases or decreases depends on the size of the remaining factors.

4. Experimental techniques

4.1 Materials

Looking at skin in a technical way, one perceives a material that is build up of a fibre-reinforced bottom layer (dermis) and a thinner upper layer (epidermis) with the stratum corneum as a stiff top part. This combination of layers is anisotropic, has a non-linear force-displacement relationship and is visco-elastic. This last property is very important and should be taken into account when attempting to model skin. Considering non-biological materials for a physical model, it shows that soft rubbers also show visco-elastic material behaviour and so rubbers were used to produce an artificial skin. Analogous to skin the artificial skin was build up with different layers: a very soft sticky silicon rubber layer on the bottom (Silgel 612 Wacker Chemicals mix ratio A:B=1:1) and a stronger less sticky silicon rubber at the top (Silgel 601 Wacker Chemicals mix ratio A:B=9:1). The silicon rubbers consist of two components, which start to harden

	thickness 612 layer	thickness 601 layer	profile obtained from	tray
S 612	7.6 mm	-	-	C
S 601	-	7.6 mm	-	C
C 13	< 7.6 mm	>> 0.66 mm	foil, circular and groovy holes	C
C 14	7.6 mm	<< 0.66 mm	foil, circular and groovy holes	C
C 15	7.6 mm	≤ 0.66 mm	foil with circular holes	C, R
C 16	7.6 mm	≤ 0.66 mm	tissue	C, R

Table 1 Used test materials

when they get in touch with each other. This hardening process takes about 1 hour at 65 °C for a one centimetre thick layer.
Skin surface isn't smooth, it has profile. So different profiles were applied in the top layer. The profiles were obtained of two foils of shaving apparatus and precision wipers (Kimwipes, Kimberley-Clark). Foil with circular holes and foil with circular and slot holes were used (Figure 4).
The soft layer was placed and hardened before the top layer and the foil or tissue were placed. The bond between the two layers was very strong. After the whole hardened, the foil or tissue were removed. The used test materials are given in Table 1. The thickness of the basic layer was pretty well controlled. Controlling the thickness of the top layer caused problems. It varies from place to place in one test object. An other problem is that the rubber of the top layer can flow through the openings of the foil. After removing the foil, a certain weight of Silgel 601 is lost and the profile is not uniform. This makes it more complicated to interpret the results measured for the mechanical properties.
For the different measurements two different trays were applied: a cylindrical tray (C) with a diameter of 50 mm for rotation friction measurements and indentation tests and a rectangular tray (R) with a bottom area of 40 and 200 mm for translation friction measurements.

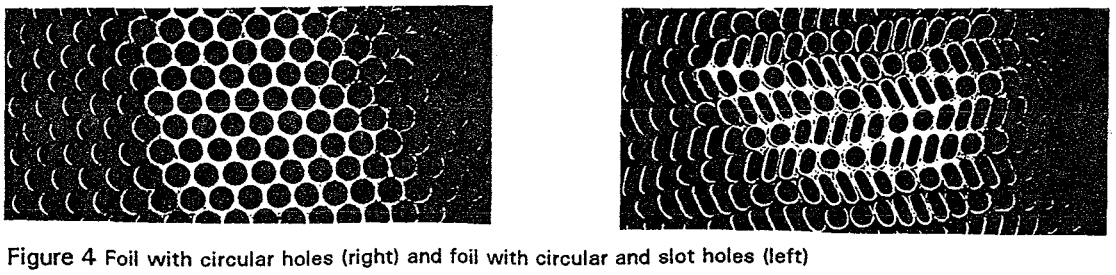

Figure 4 Foil with circular holes (right) and foil with circular and slot holes (left)

4.2 Methods

Stationary friction is measured with the rotation friction meter. During this measurement the probe causes a static indentation. To determine the quasi static indentation characteristics measurements were done with the Electro Dynamo Meter (EDM). Besides this elastic behaviour the rubber combinations have viscous properties. To learn something about these dissipative properties dynamic indentation tests were done with the EDM, but the frequency domain is very limited with this apparatus. So besides measurements were done with the Skin Impedance Meter (SIM). To simulate more realistic movements, translation friction tests were done.

4.2.1 Rotation friction

Rotation friction was measured with an apparatus with a rotating probe (Figure 5). This probe was pushed against the test material with a normal force of about

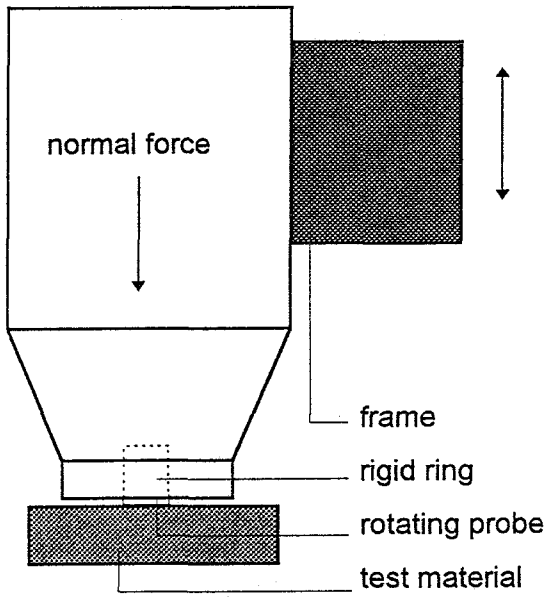

Figure 5 The rotation friction meter

40 mN. The probe had a radius of 5 mm and a rotation frequency of 1.6 Hz. To obtain a uniform contact pressure between probe and test specimen, a rigid ring was placed around the probe resulting a more or less flat contact surface. The moment and normal force on the probe were measured. It can be written for the moment:

$$M = \int_0^{2\pi}\int_0^{R} \tau(r) r^2 dr d\varphi$$

in which R is the radius of the probe and $\tau(r)$ is the shear stress. Assuming that the shear stress τ is proportional with the friction coefficient f and the normal stress σ, which is assumed to be independent of r and φ, it results:

$$M = \frac{2}{3}\pi f \sigma R^3$$

Whit the normal force according to:

$$W = \pi R^2 \sigma$$

it follows for the friction coefficient:

$$f = \frac{3}{2R}\frac{M}{W}$$

4.2.2 Static indentation test

The indentation characteristics were measured with the EDM (Electro Dynamo Meter) (Vos 1988) (Figure 6). This measuring equipment was equipped with a flat cylindrical probe, fixed on a thin pin. This pin transduces the generated force. The excitation of the pin is measured by a displacement transducer. Two kinds of measurements were carried out with the EDM: a static and a dynamic

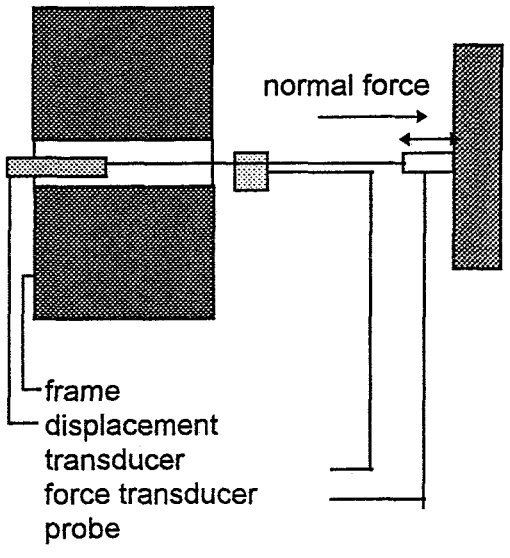

Figure 6 The Electro Dynamo Meter

measurement.

For the static measurements, the force was raised linear in ten steps from 10 to 100 mN. Each loadstep took about 12 seconds. With the EDM quasi-static experiments were done on S612, S601, C13, C14, C15 and C16. The static forces and indentations were processed and stored. The indentation characteristics were analysed by means of a spreadsheet program.

4.2.3 Dynamic indentation test

Dynamic measurements with the EDM

Besides a static load an additional alternating load can be applied with the EDM, schematically drawn in Figure 6. Such dynamic measurements with the EDM were applied to S612, S601, C14, C15 and C16. During dynamic measuring the static force was constant 50 mN. For most test materials the amplitude $S_{amplitude}$ of the sinusoidal displacement was prescribed at 0.05 mm. Only Silgel 601 was too stiff to be excitated so much, so for this test material the prescribed amplitude was taken at 0.01 mm. For later purpose it can be mentioned that Bosma (1988) measured with the EDM the dynamic characteristics of skin of the middle of the cheek. The static load in his experiment was 20 mN and the displacement amplitude was 0.1 mm. The force amplitude $F_{amplitude}$ was measured and with this information it is possible to calculate the dynamic modulus defined by:

$$C^{s}_{dynamic} = \frac{F_{amplitude}}{S_{amplitude}}$$

And the phase angle ϕ_S between the phase angle $\phi_{Famplitude}$ of the sinusoidal force signal and the phase angle $\phi_{S\ amplitude}$ of the displacement signal is defined as follows:

$$\phi_S = \phi_{Famplitude} - \phi_{Samplitude}$$

Dynamic measurements with the SIM

The Skin Impedance Meter consists (Thiel 1995) of a frame in which a mobile part is housed, see Figure 7. The mobile part can excitate randomly or sinusoidally through an air bearing. The mobile part is connected with a flat cylindrical probe with a diameter of 3 mm. The housing contains an acceleration

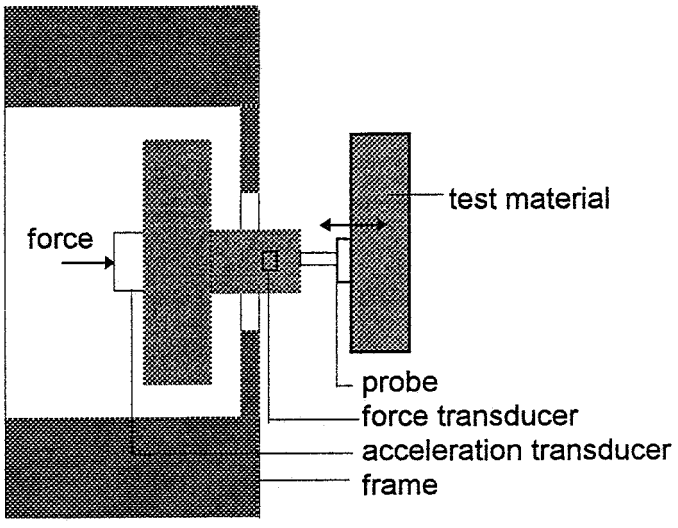

Figure 7 The Skin Impedance Meter

transducer and a force transducer. By means of the amplitude of the normal force $F_{amplitude}$ and the amplitude of the acceleration $a_{amplitude}$ the gain G is defined as:

$$G = \frac{F_{amplitude}}{a_{amplitude}}$$

and the phase angle ϕ_a between the phase angle $\phi_{Famplitude}$ of the force signal and the phase angle $\phi_{a\ amplitude}$ of the acceleration signal is defined as follows

$$\phi_a = \phi_{Famplitude} - \phi_{a\ amplitude}$$

4.2.4 Translation friction

The available measuring equipment contained a translating arm on which a 30 mm broad probe with a cylindrical ending (radius 6 mm) was fixed (Figure 8). The probe was pushed in test material and skin with a normal force of about 0.5 N and translated in a reciprocating manner and a translation distance of 5 cm. The translation velocity was fixed at 1.2 cm/s.

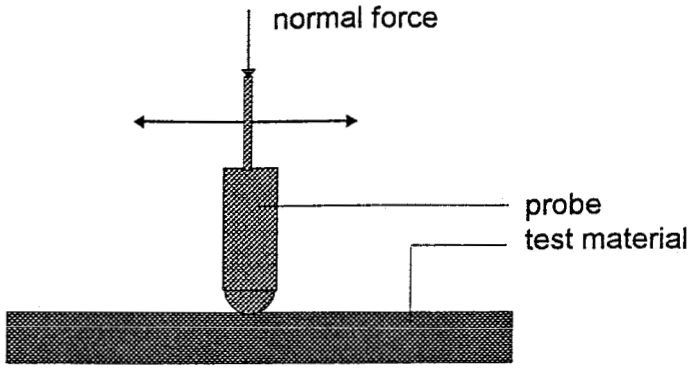

Figure 8 The translation friction meter

The friction coefficient can be defined as the ratio of the friction force $F_{friction}$ and the normal force W:

$$f = \frac{F_{friction}}{W}$$

Both $F_{friction}$ and W are measured by means of a load cell.

4.2.5 Measuring actual contact area

As appears from the previous chapter the actual contact area is expected to play a considerable part in the total friction force. With increasing actual contact area the hysteresive friction force decreases but on the other hand the adhesive friction force increases. So knowing the actual contact area could help to distinguish which kind of friction increases and which kind of friction decreases between certain experiments.
However measuring the actual contact area was not as simple as it seemed to

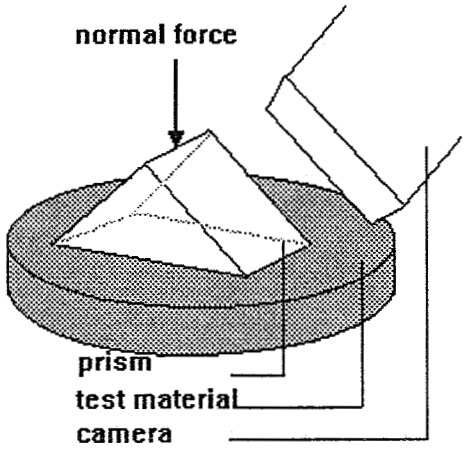

Figure 9 A possible measure equipment for measurements of the actual contact area

be. The target was to make the actual contact area visible while the test material was loaded by the same load and the same apparent contact area as in the rotation friction. The influence of movement on the actual contact area was neglected for the time being. Attempts to make it visible with ink and water vapour didn't succeed. Finally experiments were done in which a glass prism was pushed against the test material (Figure 9). Through differences in light breaking between contacted and non-contacted glass surface parts the contact area was visible, but only at the prism edges contact between prism and test

material was noticed. This was caused by peak stresses at the prism edges. It is expected that when the material around the prism is suppressed by a rigid body, one can see the actual contact area which gives an indication for the actual contact area in the rotation friction measurements. The actual contact area can be recorded with a computer camera and with special image processing software processing software the actual contact area can be count. To build the needed instruments and to measure with them would have taken too much time for the current project.
To get a rough indication of the possible actual contact area in the rotational friction experiments, profiles of the foils with which the artificial skin surface profiles were obtained on the rubber combinations (Figure 4) were recorded with a video camera. A software package was used to count the open area. This was not possible with the precision wiper profile.

5. Results

5.1 Rotation friction

Experiments were carried out to determine the rotation friction as described in Section 4.2.1.. Rubber combinations without any kind of profile have an

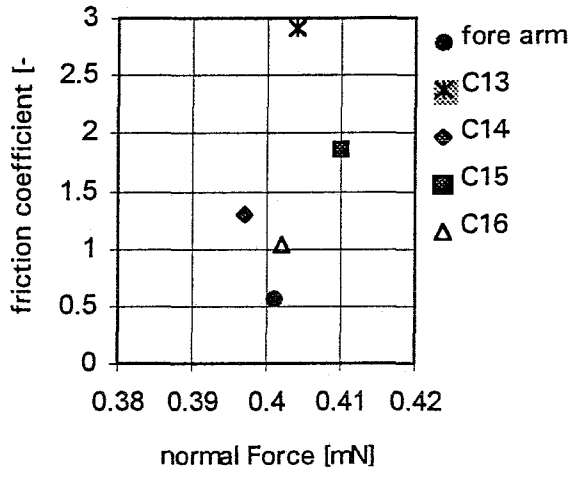

Figure 10 The results of measurements of the rotational friction

unmeasurable high and very inconstant friction. So we only measured on rubber combinations with profile. Bounded friction values were measured on C13, C14, C15, C16 and the fore arm. All the rubber combinations have a larger rotation friction coefficient (Figure 10) than the skin on the inner fore arm. From C16, C14, C15 to C13 the friction coefficient of the rubber combination rises.

5.2 Static indentation test

Static indentation tests, as explained in Section 4.2.2., were performed with the soft rubber (Silgel 612), with the stiff rubber (Silgel 601) and with all the rubber combinations mentioned in Section 4.1. The indentation characteristics of human cheek were obtained before with the EDM by Bosma (1988). It can be seen from figure 11 that Silgel 612 is very weak and Silgel 601 is very stiff. The rubber combinations have all a characteristic that lies between these two. The stiffness of the rubber combinations rises from C14 to C16, C15 and C13. Skin is even weaker than Silgel 612, but it shouldn't be set too much value on this skin characteristic, because this characteristic is measured on only one place on one person.

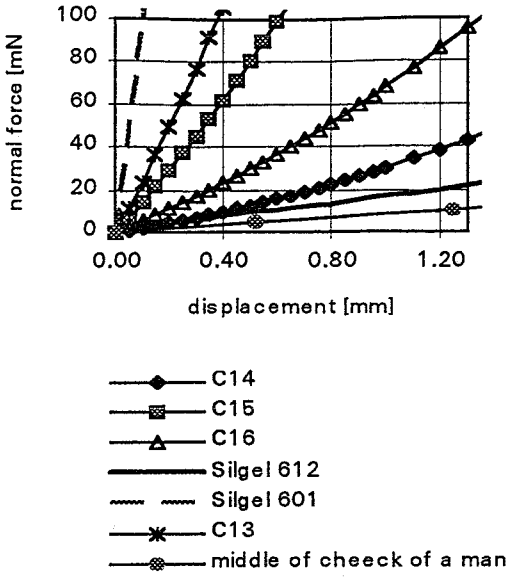

Figure 11 Results of the quasi-static indentation test with the EDM

5.3 Dynamic indentation

EDM

Measurements have been performed as described in Section 4.2.3 on Silgel 612, C14, C16, C15 and Silgel 601. The dynamic modulus increases in this order and

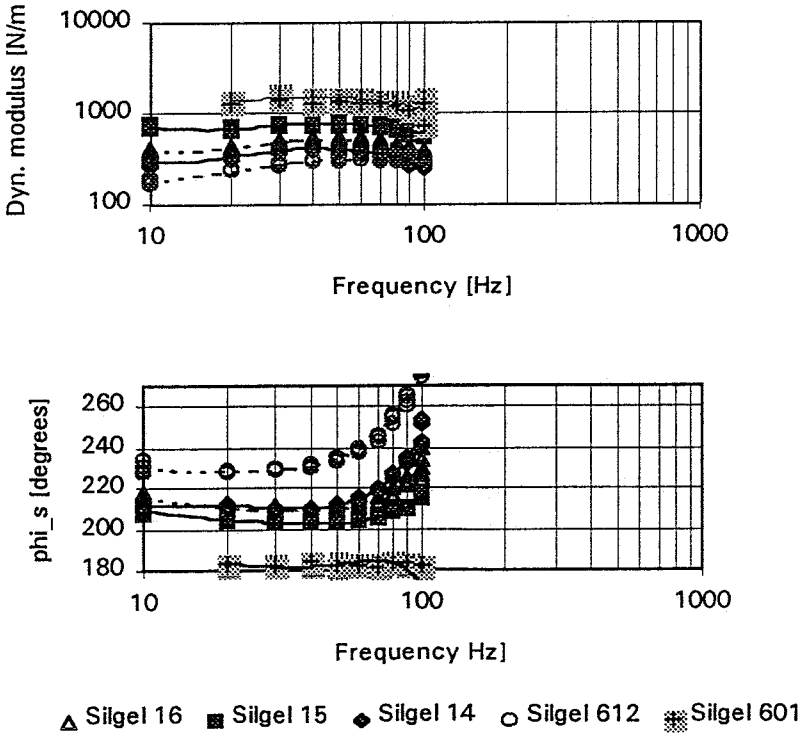

Figure 12 Results of dynamic indentation tests with the EDM

the phase angle decreases in this order (Figure 12). So the stiffer test materials (high dynamic modulus) have a smaller loss modulus (phase angle). To obtain the right phase angles 180 ° has to be substracted from the values measured by the EDM. This difference could be caused by a wrong connection of the load cells. In dynamic indentation tests on different body sites with the EDM different characteristics were found (Savenije 1988). This is shown in Figure 13.

SIM

The measurement data gathered with the SIM have been drawn logarithmic in Figure 14. The same test materials were used as for the dynamic EDM measurements. Differences between the materials appear most apparent in the phase angle. The phase angle φ_a rises from Silgel 601, C13, C15, C16, C14 to Silgel 612. To compare the phase angles obtained from the EDM to these measurements 360° has to be subtracted on account of a different defenition. The value G of Silgel 601 is higher than that of the other test materials, that differ very little from each other. The G characteristics have a direction coefficient of about -2. This would be with EDM measurements about zero (horizontal line) and Figure 12 confirms this roughly. To compare G and $C^s_{dynamic}$ the following rectangular relationship can be used in which freq is the indentation frequency:

$$G = \frac{C^s_{dynamic}}{4\pi^2 freq^2}$$

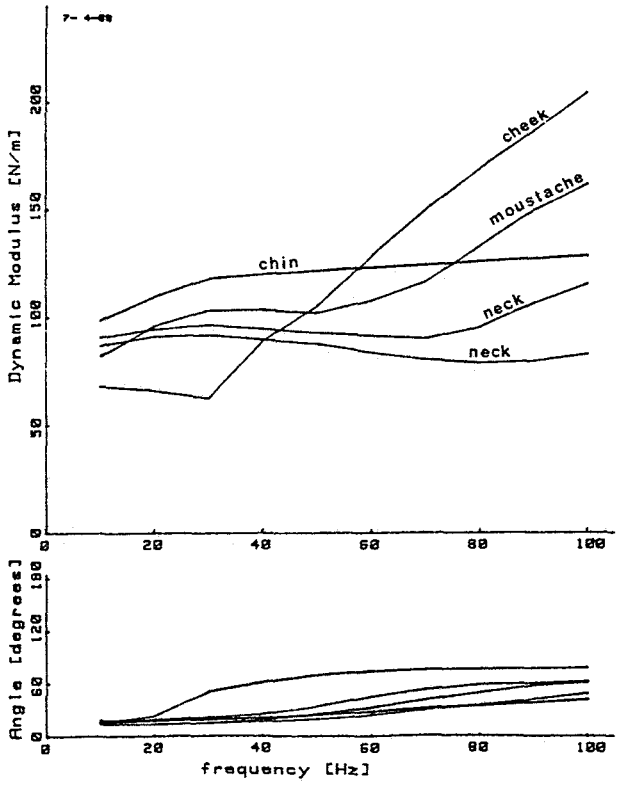

Figure 13 Results of dynamic indentation tests with EDM performed on skin (Savenije 1988)

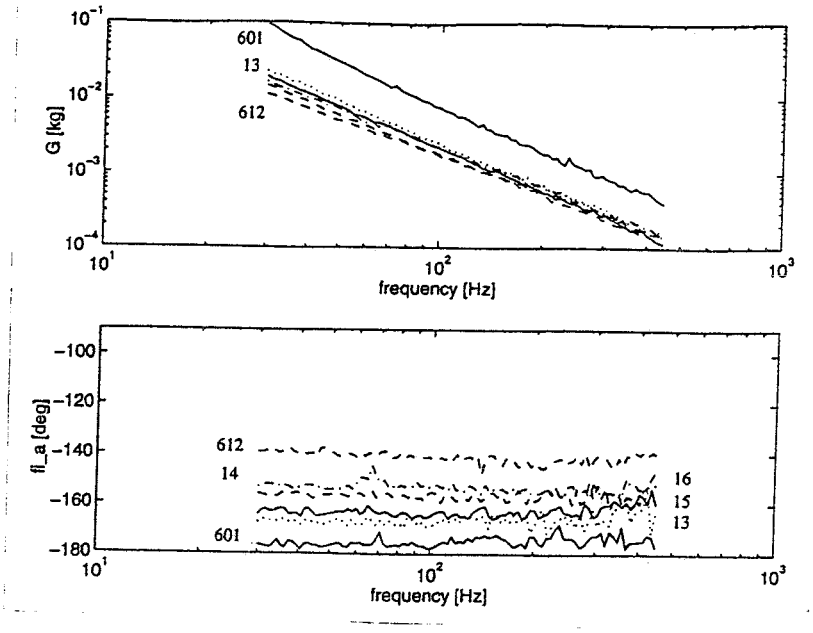

Figure 14 Results of dynamic measurements with SIM

Translation friction

For doing translation friction measurements only two test materials were available in rectangular trays: R15 and R16. The layers had about the same thickness as in the circular trays. Besides these test materials, skin of the inner fore arm was tested. The two test materials had a translation friction coefficient that was 1.5 to 2 times higher than that of skin. R15 had the highest translation friction coefficient (Figure 15).

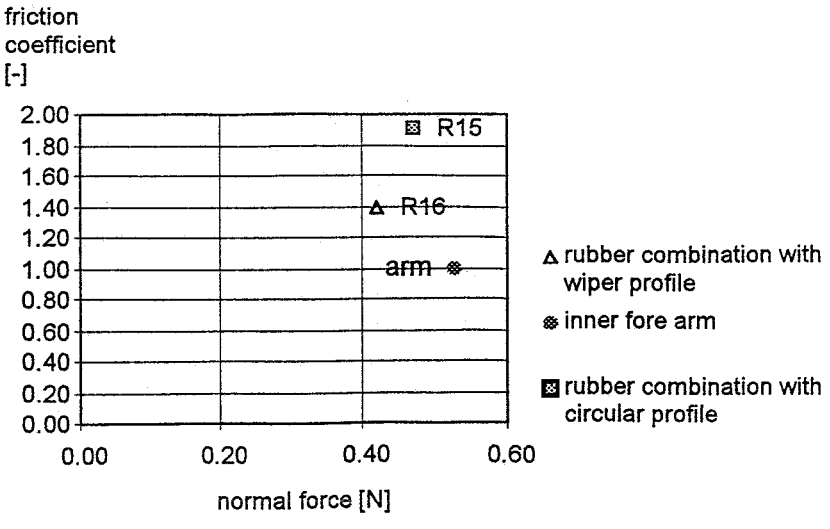

Figure 15 Results of translations friction experiment

5.5 Measuring real contact area

As indicated before a realistic measurement of the actual contact area wasn't realised yet. Therefor the foils, which were used for obtaining the test materials' surface profile, were recorded. With the software package 'Quantimet' the density of openings was determined. The foil with circular holes had 65% openings and the foil with slot shaped holes had 51% openings, which is used as an indication for the actual contact area in the rotation friction measurements.

6. Discussion

6.1 Rotation Friction

Considering the rotation friction coefficients of C14 and C13 large differences are observed, although the profile is obtained from the same foil. As mentioned in Section 4.1 it is possible that some of the upper layer disappears through the holes of the foil, used for obtaining profile on the surface of the test material. This occurred when C14 was prepared, but when C13 was prepared this wasn't observed. The C13 profile is more or less parabolic, but the profile of C14 isn't when viewed by microscoop. Its profile seems to have flat tops. So the profiles of C13 and C14 seem to differ. Beside the different profile there seems to be an other factor which is involved in determining the rotational friction coefficient. This will be discussed next.

6.2 Static indentation

Different layer thickness' were observed in C13 and C14. C13 had a less thick weak basic layer and a thicker stiff upper layer than C14. So according to this it is expected that C13 as a whole is stiffer than C14. To determine the influence of the stiffness on the friction coefficient the indentation test was applied. From the static indentation test it is indeed learned that C13 is much stiffer than C14. C15 has an indentation characteristic that lies between C14 and C13 and the rotation friction coefficient lies also between the rotation friction coefficient of C14 and C15. So from this it can be hypothesised that the friction coefficient and the indentation characteristic are related. But test material C16 doesn't confirm this relationship. C16 has an indentation characteristic that lies between C14 and C15, but the rotation friction coefficient is lower than C14 and C15. Probably the characteristic of the surface plays also a part. The surface of C16 has a profile obtained from wipers and it contains small fibres which become visible when examined through the microscope. These small fibres might cause the adhesion friction to reduce, because there isn't adhesion between fibres of the wiper and the probe.

6.3 Dynamic indentation

Dynamic indentations have been measured with two apparatus: the EDM and the SIM. Although definitions of the graphs obtained from these experiments differ, the phase angle characteristics can easily be compared, because only a vertical shift is needed. In the two phase angle graphs the order of test materials is the same, but the shapes are considerably different. The phase angle characteristics obtained from the SIM are more or less horizontal, but the dynamic EDM phase angle characteristics on the other hand turn off to larger phase angle. This starts at 50 Hz. Until 50 Hz the characteristics are more or less flat. This curve in the phase angle characteristic is not found in dynamic characteristics measured by the SIM. It could be a result of the different ways the apparatus work. The EDM prescribes a constant displacement amplitude. Through this the accelerations at high frequencies become high. It is possible that the EDM make large faults through this, but it is also possible that the phase angle is dependent on the acceleration amplitude. The SIM prescribes a constant acceleration amplitude. The displacement amplitude is very small at high frequencies through this.

6.4 Translation friction

The rubber combinations (R15 and R16) used for translation friction tests had the same layer thickness'. However the translation friction coefficients differ much. The translation friction coefficient of R16 (with profile obtained from wipers) was about two third of the coefficient of R15 (with profile obtained from foil with circular holes). It is possible that the lower indentation stiffness of R16 is related to the lower friction coefficient. But this lower friction coefficient could also be caused by less adhesion through the presence of the small wiper fibres.

6.5 Measuring the actual contact area

The openness of the foils which were used to obtain profile, were measured. This number gives only a very rough overrating of the actual contact area. These values could be used as a upper limit of the actual contact area. The test materials with the circular and slot holes had different layer thickness', which may be of influence on the actual contact area through the resulting stiffness differences. So it would be too premature to conclude something from these measurements with respect to the influence of the used foil on the friction.

6.6 Friction theory

The theory described in section 3 divides the friction into an adhesive and a hysteresive part. The adhesive friction includes the stick effect between test material and probe. Hysteresive friction can be caused by a probe which ploughs through the test material.
Considering the roughness of the test materials used, the roughness of the translating and the rotating probe are negligible. So it is reasonable to suppose that ploughing by the roughness of the probe doesn't occur and thus not results in deformative friction.
After the rotation friction meter runs a while a stationary situation is created. The test material is deformed by a static normal force and it is reasonable to assume that it doesn't contribute to the deformation friction, because the deformation field is supposed to be quasi-static. So only adhesive friction is expected to appear in rotation friction experiments.
Translation friction experiments on the other hand do have hysteresive friction. The translation of the probe causes a large deformation, because it pushes a material lump in front of it. Adhesion between probe and test material is plausible. So in the translation friction test, adhesion friction as well as hysteresive friction is assumed to appear.
If it is assumed besides the above assumptions that in spite of the different probes, different test samples and the different normal loads the adhesive friction coefficient is the same in the rotation and translation friction experiments, the differences between the translation and rotation friction

	$f_{rotation}$	$f_{translation}$	$f_{translation} - f_{rotation}$
C15	1.8	1.9 *	0.1 *
C16	1.0	1.4	0.4
skin	0.5	1.0 *	0.5

Table 2 Different friction coefficients

coefficient must be the hysteresive friction coefficient. In table 2 this is restored The values of C15 with a star behind are not reliable, because they were

* see text

measured while a the upper surface was preloaded. This was necessary, because the surface was wrinkled (origin unknown) and that heightened the friction very much (translation friction coefficient up to 50). When the surface was preloaded the translation friction coefficient was measurable, but this caused probably the friction coefficient to lower, as in this case deforming of the test material was more difficult and thus the deformation friction lowered. From table 2 one can conclude that the translation friction coefficient is indeed higher than the rotation friction coefficient for the tested materials and skin. So this doesn't reject the theoretical suppositions made above, but it doesn't prove these theories.

7. Conclusions

Some properties of rubber combinations and skin have been tested.

- The rotational and translational friction of skin and rubber combinations are not the same, but they are of the same order. A large dependence on layer thickness is perceived.
- The influence of the profile type on the surface could not be determined very well with the experimental techniques used. However indication exist that the kind of profile is not a the only factor, but also the stiffness of the rubber combinations plays a role. To obtain a moderate friction it is important that the surface has some kind of profile.
- Rubber combinations are much stiffer than that of skin (at least three times) when measured with quasi-static and dynamic indentation tests.
- Compared to skin the dynamic modulus of the test materials are high (up to ten times).

8. Recommendations

A rubber combination is a complicate mechanical system, that is dependent on different factors. To learn more about this system further research is required. The same applies for skin. When the mechanical systems of skin and rubber combinations are known pretty well one could build an artificial skin in a more structural way by searching the right rubbers and try to adapt the mechanical properties of the rubber combinations to these of skin.
This report contains only a preparatory study to the main lines of macroscopic contact behaviour. Many factors of interest have been left out of consideration, like:

- the dependency of rotation and translation friction on the normal force
- the in-plane stiffness
- the dependency of rotation and translation friction on velocity
- the influence of the geometry of the tray
- the influence of the material of the probe
- the influence of environmental factors like humidity and temperature

in which the factor mentioned first is probably the most important.

To be able to do more structural research the procedure to obtain test materials has to be optimised. It should be required from a new procedure that:

- the thickness of the layers is uniform and exactly known
- it should be possible to produce a very thin upper layer (to obtain better results with indentation tests)
- the profile has to be uniform and the exact shape of the profile should be known

A solution to these problems could be the following procedure: First prepare the Silgel 601 and pour this into a mould with the desired profile on the bottom, then push a stamp against the Silgel 601 until it has hardened. After that pour the Silgel 612 into the mould and let it harden with a stamp on it. The height of the stamp should be accurate adjusteable.
To improve the understanding of the physical phenomena, measuring of the actual contact area is required. With the present experimental techniques this was not possible and so a technique should be developed as described in Section 4.2.5..

9. Literature

- Bartenev G.M., Lavrentev V.V., *Friction and wear of polymers,* Elsevier, Amsterdam, 1981
- Bosma H., Vos de R., *Mechanical properties of human skin, Measurements I,* Philips Report nr. 6264, 1988
- Gerrard W.A., *Friction and other measurements of the skin surface,* Bioeng. Skin 3, pages 123-139, 1987
- Johnson S.A., Gorman D.M., Adams M.J., Briscoe B.J., *The friction and lubrication of human stratum corneum,* Thin films in tribology, Elsevier, Amsterdam, 1993
- Moore D.F., *Principles and applications of tribology,* Pergamon Press Ltd. Oxford 1975
- Savenije E.P.W., *Structure and mechanical properties of human hair and skin,* Philips Report nr. 5806, 1982
- Savenije E.P.W., Vos de R., *Mechanical properties of human skin,* Philips Report nr. 6264, 1988
- Shimi A.F., *In vivo skin friction measurements,* J.Soc.Cosmet., Chem., 28, pages 37-51, february 1977
- Stachowiak G.W., Batchelor A.W., *Engineering tribology,* Elsevier, Amsterdam, 1993
- Thiel J.L., *Skin and hair dynamics, for purpose of epilation,* WFW report, Eindhoven University of Technology., Eindhoven, 1995
- Vos R., *The mechanical properties of human skin, user guide for the EDM,* Philips technical note nr. 078/88, 1988